Electric circuit networks equivalent to chaotic quantum billiards

Evgeny N. Bulgakov,[1,3] Dmitrii N. Maksimov,[1] and Almas F. Sadreev[1,2,3]
[1]*Kirensky Institute of Physics, 660036 Krasnoyarsk, Russia*
[2]*Department of Physics and Measurement, Technology Linköping University, S-581 83 Linköping, Sweden*
[3]*Astaf'ev Pedagogical University, 660049 Lebedeva, 89, Krasnoyarsk, Russia*
(Received 4 November 2004; published 11 April 2005)

We consider two electric *RLC* resonance networks that are equivalent to quantum billiards. In a network of inductors grounded by capacitors, the eigenvalues of the quantum billiard correspond to the squared resonant frequencies. In a network of capacitors grounded by inductors, the eigenvalues of the billiard are given by the inverse of the squared resonant frequencies. In both cases, the local voltages play the role of the wave function of the quantum billiard. However, unlike for quantum billiards, there is a heat power because of the resistance of the inductors. In the equivalent chaotic billiards, we derive a distribution of the heat power which describes well the numerical statistics.

DOI: 10.1103/PhysRevE.71.046205 PACS number(s): 05.45.−a, 03.65.Ge, 03.65.Yz

I. INTRODUCTION

Electric circuit models representing a quantum particle in the one-dimensional potential

$$-\frac{\hbar^2}{2m}\frac{\partial^2\psi(x)}{\partial x^2}+V(x)\psi(x)=E\psi(x) \tag{1}$$

were considered first by Kron in 1945 [1]. Here, three equivalent circuits were treated. The first one contained positive and negative resistors, and in each state the currents and voltages were constant in time. The second and third circuits were similar to one another. They consisted of inductors and capacitors, and the currents and voltages were sinusoidal in time. In the same year 1945, Carter and Kron [2] performed tests of one-dimensional circuits. Measurements were made of eigenvalues and eigenfunctions for the particular cases of the harmonic oscillator, the rectangular potential well, the double rectangular barrier, the single barrier, and the rigid rotator. Recently large random *RLC* networks with a random mixture of capacitances and inductances [3] were intensively studied with application to many physical phenomena (see [4] and references there). In particular, it was shown that fluctuations in the spectra are described well by the random matrix theory [4].

Here we consider the stationary Schrödinger equation in two-dimensional billiards in the hard wall approximation,

$$-\nabla^2\psi(x,y)=\epsilon\psi(x,y), \tag{2}$$

where the Dirchlet boundary condition is implied at the boundary C of the billiard:

$$\psi_C=0. \tag{3}$$

We use Cartesian coordinates x,y which are dimensionless via a characteristic size L of the billiard. Further $\epsilon=E/E_0$, $E_0=\hbar^2/2mL^2$.

Real quantum billiards might been realized as quantum dots. However, studies are difficult to perform because of many experimental demands. First, one has to manufacture the billiards as quantum dots, which is hard but possible. Second, the studies might be obscured by Coulomb and electron-phonon interactions. Third, there is an error in the measurements of the eigenfunctions by the scanning tunneling microscopy technique. Fortunately, nowadays there are physical systems which are mathematically equivalent or similar to quantum billiards. First, there is a complete equivalence of the two-dimensional Schrödinger equation for a particle in the quantum billiard to the microwave billiards [5]. The wave function corresponds exactly to the electric field component of the TM mode of electromagnetic field: $\psi(x,y)\leftrightarrow E_z(x,y)$ with the same Dirichlet boundary conditions. This equivalence turned out to be very fruitful and allowed one to test a lot of predictions in the quantum mechanics of billiards [6–8]. Second, we refer to experiments on elastomechanical wave functions in chaotic plates [9–11], which present an acoustic wave analog for quantum billiards.

On the other hand, there are models for the equivalent *RLC* circuit of a resonant microwave cavity which establish an analogy near an eigenfrequency [12]. Manolache and Sandu [13] proposed a model for a resonant cavity that is associated with an equivalent circuit consisting of an infinite set of coupled *RLC* oscillators. Therefore, there is a bridge between quantum billiards and a set of coupled *RLC* oscillators [14]. In fact, we show here that, at least, two models of electric resonance circuits (ERCs) can be proposed. In the first model shown in Fig. 1, the eigenfunctions correspond to voltages and the eigenenergies to the squared eigenfrequencies of the ERC. In the second model shown in Fig. 2 the eigenenergies of the quantum billiard correspond to the inverse of the squared eigenfrequencies of the electric network. The electric network analog systems allow us to measure not only typical quantum variables such as the probability distribution and probability current but also the distribution of the heat power in chaotic billiards. Moreover, the intrinsic resistances of the *RLC* circuit allow one to model decoherence processes.

II. EQUIVALENCE BETWEEN ELECTRIC RESONANCE CIRCUITS AND QUANTUM BILLIARDS

In order to map the two-dimensional Schrödinger equation onto the numerical grid $(x,y)\Rightarrow a_0(i,j)$, $i=1,2,\ldots N_x$, j

 ©2005 The American Physical Society

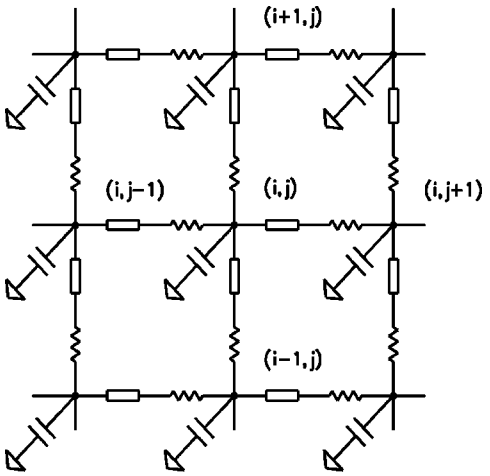

FIG. 1. The first model of resonance *RLC* circuits.

$=1,2,\ldots N_y$ with a_0 as the elementary unit length of the grid, we write the operator ∇^2 in the finite difference element approximation [15]

$$\nabla^2\psi_{ij} \approx \frac{\psi_{i,j+1}+\psi_{i,j-1}+\psi_{i+1,j}+\psi_{i-1,j}-4\psi_{i,j}}{a_0^2}.$$

Then the the Schrödinger equation (2) takes the following form:

$$\psi_{i,j+1}+\psi_{i,j-1}+\psi_{i+1,j}+\psi_{i-1,j}+(a_0^2E-4)\psi_{i,j}=0. \quad (4)$$

Let us consider the electric resonance circuit shown in Fig. 1. Each link of the two-dimensional network is given by the inductor L with the impedance

$$z_L = i\omega L + R \quad (5)$$

where R is the resistance of the inductor and ω is the frequency. Each site of the network is grounded via the capacitor C with the impedance

$$z_C = \frac{1}{i\omega C}. \quad (6)$$

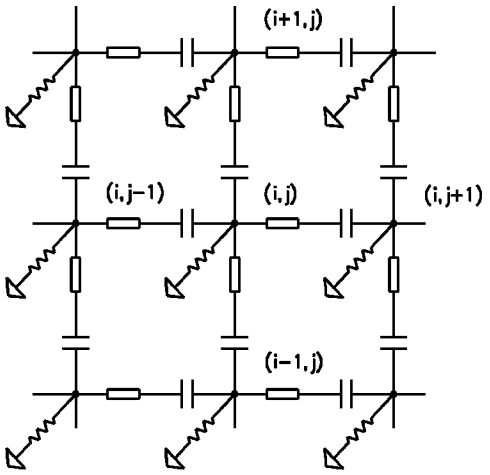

FIG. 2. The second model of resonance *RLC* circuits.

Kirchhoff's current law at each site of the network gives

$$\frac{1}{z_L}[V_{i,j+1}-V_{i,j}+V_{i,j-1}-V_{i,j}+V_{i+1,j}-V_{i,j}+V_{i-1,j}-V_{i,j}] - \frac{1}{z_C}V_{i,j}=0, \quad (7)$$

where $V_{i,j}$ is the voltage at the site (i,j). One can see that this equation coincides with the discretized version of the Schrödinger equation (4) with $V_{i,j}$ as $\psi_{i,j}$ and the eigenenergies as

$$a_0^2k^2 = -\frac{z_L}{z_C} = LC\omega^2 - iRC\omega = \frac{\omega^2}{\omega_0^2} - i\frac{\gamma\omega}{\omega_0^2}, \quad (8)$$

where $\omega_0=1/\sqrt{LC}$ and $\gamma=R/L$ are, respectively, the eigenfrequency and the linewidth of each resonance circuit.

For the second network of electric resonance circuits shown in Fig. 2 we obtain

$$\frac{1}{z_C}[V_{i,j+1}-V_{i,j}+V_{i,j-1}-V_{i,j}+V_{i+1,j}-V_{i,j}+V_{i-1,j}-V_{i,j}] - \frac{1}{z_L}V_{i,j}=0. \quad (9)$$

Comparing this equation with Eq. (4) we have

$$a_0^2k^2 = -\frac{z_C}{z_L} = \frac{1}{LC\omega^2} + \frac{iR}{L\omega} = \frac{\omega_0^2}{\omega^2} + i\frac{\gamma\omega_0^2}{\omega} \quad (10)$$

where $\gamma=RC$. It is surprising, that the eigenvalues of the quantum billiard are the inverse of the resonant frequencies of the equivalent electric network that is shown in Fig. 2. This network opens therefore the interesting possibility of studying the high eigenvalues of the quantum billiard by applying a low frequency ac voltage. There is, however, a limit for the frequency $\omega \gg \omega_0$ because of the coarseness of the network's grid.

There are many ways to define the boundary conditions (BCs). Let (i_C,j_C) be the sites that belong to the boundary of the network. If these sites are grounded, we obtain obviously the Dirichlet BCs (3) $V_{|C}=0$. If they are shunted through capacitors we obtain the free BCs (the Neumann BCs). Moreover, if the boundary sites are shunted through resistive inductors, the BCs correspond to mixed ones.

III. ANALOG TO THE CHAOTIC BUNIMOVICH BILLIARD

A real electric circuit network has three features which cause it to have some differences from a quantum billiard. These features are (1) the discreteness of the resonance circuits, (2) the tolerance of the electric elements, and (3) the resistance of the inductors. In practice the discreteness does not have any effect for $\lambda \geqslant 10_{a_0}$ where λ is the characteristic wavelength of the wave function, and a_0 is the elementary unit of the network.

Numerically we consider an electric network with the shape of a quarter of the Bunimovich billiard. The distribu-

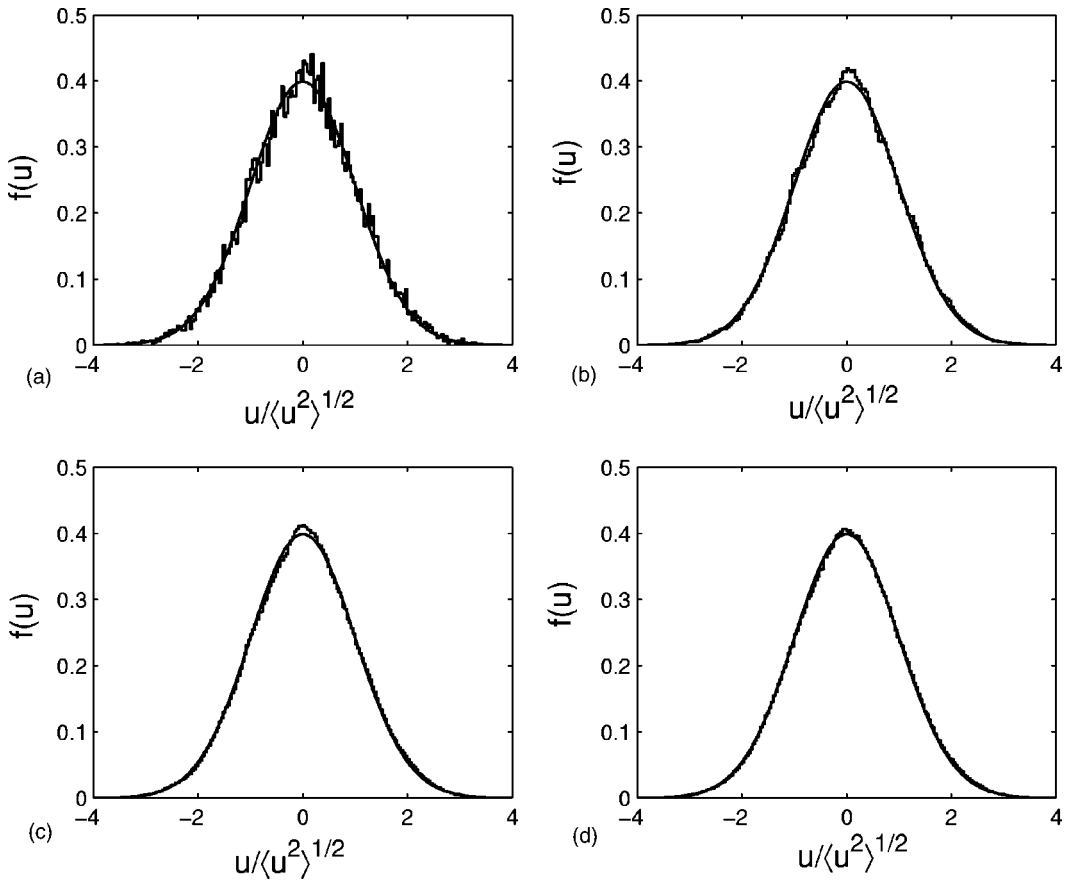

FIG. 3. The distribution of the real part of the wave function of the quarter Bunimovich billiard mapped onto the resonance *RLC* circuit with the elementary unit $a_0=0.01$, $\omega=1.722$ MHz, $L=0.1$ mH, $C=1$ nF, $R=0$. (a) There is no tolerance of the electric circuit elements; the tolerance equals (b) 1%, (c) 3%, and (d) 5%. Each distribution in (b)–(d) is averaged over 100 realizations of the electric network.

tion of the real part of the wave function of the billiard mapped onto the electric circuit network with $a_0=1/100$ is shown in Fig. 3(a). The wavelength is $\lambda=2\pi a_0\omega_0/\omega=0.115$ with the parameters given in the caption of Fig. 3. We take the width of the billiard to be 1. One sees a distinct deviation of the distribution from the Gaussian one which results from multiple interferences on the discrete elements of the network.

It is known that noise, for example, temperature, smooths the fluctuations of the transmission through quantum billiards [16,17]. In the present case the tolerance of the circuit elements, the capacity and inductance, plays the role of noise. We expect therefore that, by increasing the tolerance, we can suppress the fluctuations in the distribution of the wave function of the discrete electric circuit network. In fact, even a 1% tolerance smooths substantially the distribution of the wave function as shown in Figs. 3(b)–3(d). We consider that the fluctuations of capacitors and inductors are not correlated at different sites.

Finally we consider the distribution of the wave function of the electric *RLC* resonance circuit network when the damping is caused by the resistance of the inductors. In order to excite the network we apply an external ac current at a single site of the network. Figure 4 shows the probability density for two values of the resistance R in a quarter of the Bunimovich billiard. We see a localization effect [Fig. 4 (right)] that is caused by the damping of the probability density flowing from the ac source (see also Fig. 7 below). The characteristic localization length can be easily estimated from Eq. (8):

$$\lambda_R \approx \frac{4\pi a_0}{R}\sqrt{\frac{L}{C}}. \tag{11}$$

The distributions of the probability density $\rho=|V|^2$ for open quantum chaotic billiards have been considered in many articles [18–22] for the case of zero damping. Here we follow [22,24] and perform the phase transformation $V \rightarrow V\exp(i\theta)=p+iq$ by which the real and imaginary parts of the wave function V become statistically independent. Introducing a parameter for the openness of the billiard [24],

$$\epsilon^2 = \frac{\sigma_q^2}{\sigma_p^2}, \tag{12}$$

where $\sigma_p^2=\langle p^2\rangle$, $\sigma_q^2=\langle q^2\rangle$, we can write the distribution of the probability density as [22]

$$f(\rho) = \mu\exp(-\mu^2\rho)I_0(\mu\nu\rho) \tag{13}$$

with the following notations:

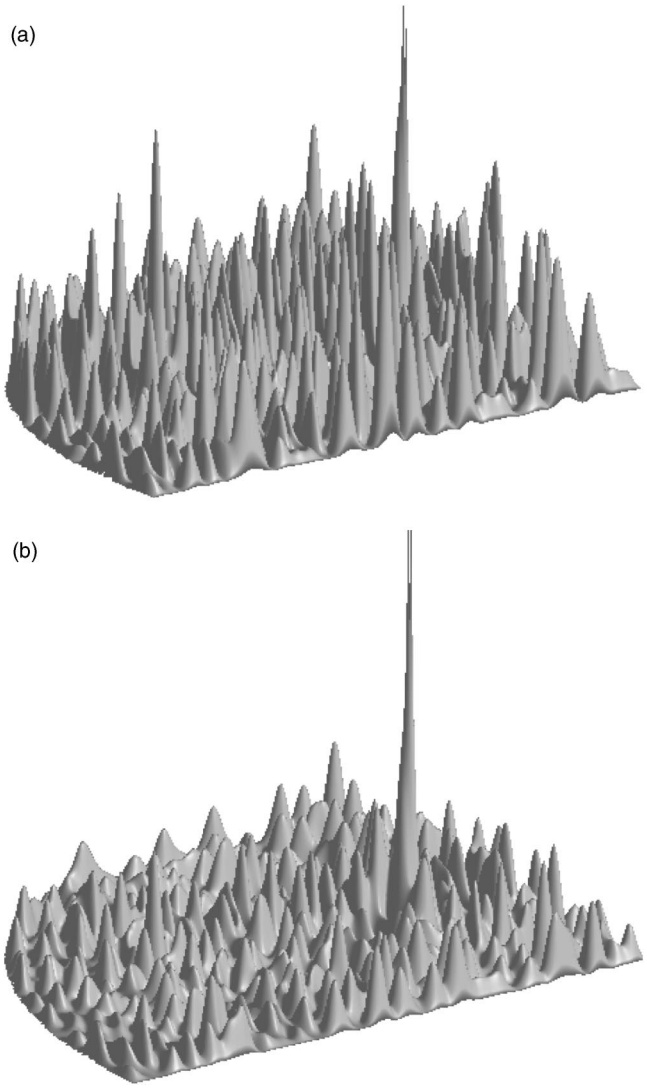

FIG. 4. Views of the probability density in the quarter Bunimovich billiard that is mapped onto the resonance *RLC* circuit with the elementary unit $a_0=0.005$, $\omega=0.8611$ MHz, $L=0.1$ mH, $C=1$ nF. Left $R=0.5\ \Omega$, right $R=1\ \Omega$. The point of connection of the external ac current is at the maximum of the probability density.

$$\mu=\frac{1}{2}\left(\frac{1}{\epsilon}+\epsilon\right),\quad \nu=\frac{1}{2}\left(\frac{1}{\epsilon}-\epsilon\right). \tag{14}$$

Here, $I_0(x)$ is the modified Bessel function of zeroth order. This distribution is shown in Fig. 5 by solid lines while the Rayleigh distribution $f(\rho)=\exp(-\rho)$ is shown by dashed lines. The Rayleigh distribution specifies the distribution of the completely opened system. One can see from Figs. 5(a) and 5(b) that the statistics of the probability density follows the distribution (13) irrespective of the resistance R. However with growing resistance, the distribution (13) tends to the Rayleigh distribution [Figs. 5(c) and 5(d)]. This tendency in the statistics of the probability density can be understood since the quantum system is more open when the resistance is larger.

IV. THE HEAT POWER

In open systems the probability current density corresponds to the Poynting vector. This equivalence allows to test, in particular, the universal current statistics in chaotic billiards [23,24]. However, in the electric resonance circuit there are heat losses because of the resistance. The local power of the heat losses is defined by [25]

$$P=\frac{R}{2}[\mathrm{Re}(I_x)^2+\mathrm{Im}(I_x)^2+\mathrm{Re}(I_y)^2+\mathrm{Im}(I_y)^2]=\frac{R}{2}[|I_x|^2+|I_y|^2], \tag{15}$$

where I_x, I_y are the local components of the electric current that flows between the sites of the electric network:

$$RI_x(i,j)=V_{i+1,j}-V_{i,j},\quad RI_y(i,j)=V_{i,j+1}-V_{i,j}. \tag{16}$$

The peculiar property of large electric networks to disperse electric power, was first noticed by Dykhne [26]. We approximate the true state with the Berry conjecture

$$V(x,y)=\sum_j a_j \exp[i(\mathbf{k}\cdot\mathbf{r}+\phi_j)] \tag{17}$$

where a_j and ϕ_j are independent random real variables and k_j are randomly oriented wave vectors of equal length. Then V is a complex random Gaussian field (RGF) in the chaotic Bunimovich billiard. The derivatives of V are also independent complex RGFs. The components I_x, I_y form two complex RGFs with the probability density of these fields

$$f(I_x',I_y',I_x'',I_y'')=\frac{1}{4\pi^2\sigma_r^2\sigma_i^2}\exp\left\{-\frac{1}{2}\left(\frac{I_x'^2+I_y'^2}{\sigma_r^2}+\frac{I_x''^2+I_y''^2}{\sigma_i^2}\right)\right\} \tag{18}$$

where $I_x'=\mathrm{Re}(I_x)$, $I_y'=\mathrm{Re}(I_y)$, $I_x''=\mathrm{Im}(I_x)$, $I_y''=\mathrm{Re}(I_y)$, $\sigma_r^2=\langle I_x'^2\rangle,\langle I_y'^2\rangle$, $\sigma_i^2=\langle I_x''^2\rangle,\langle I_y''^2\rangle$. In numerical computations we use the fact that the average over the billiard area

$$\langle\cdots\rangle=\frac{1}{A}\int d^2\mathbf{x}\cdots, \tag{19}$$

is equivalent to the average over the three complex RGFs

$$\langle\cdots\rangle=\int d^2V\, d^2I_x d^2I_y f(\mathrm{Re}(V),\mathrm{Im}(V))f(I_x',I_y',I_x'',I_y'')\cdots. \tag{20}$$

An example for the distribution of the real part of I_x is presented in Fig. 6(a) which shows that numerically this value is, in fact, a RGF. The definition of the probability distribution (18) relies on the assumption that the Berry function (17) is isotropic in space: $\langle I_x'^2\rangle=\langle I_y'^2\rangle$, $\langle I_x''^2\rangle=\langle I_y''^2\rangle$. The space anisotropy of the shape of the billiard affects the statistical anisotropy. However this effect is caused by the boundary condition and is of the order of $L_P\lambda/A\sim\lambda$. Here L_P is the length of the billiard perimeter, and λ is the characteristic wavelength of the wave function in terms of the width of the billiard. Therefore, for the excitation of the eigenfunction with sufficiently high frequency we can use the distribution function (18). The numerically computed mean values, given in Table I, confirm this conclusin.

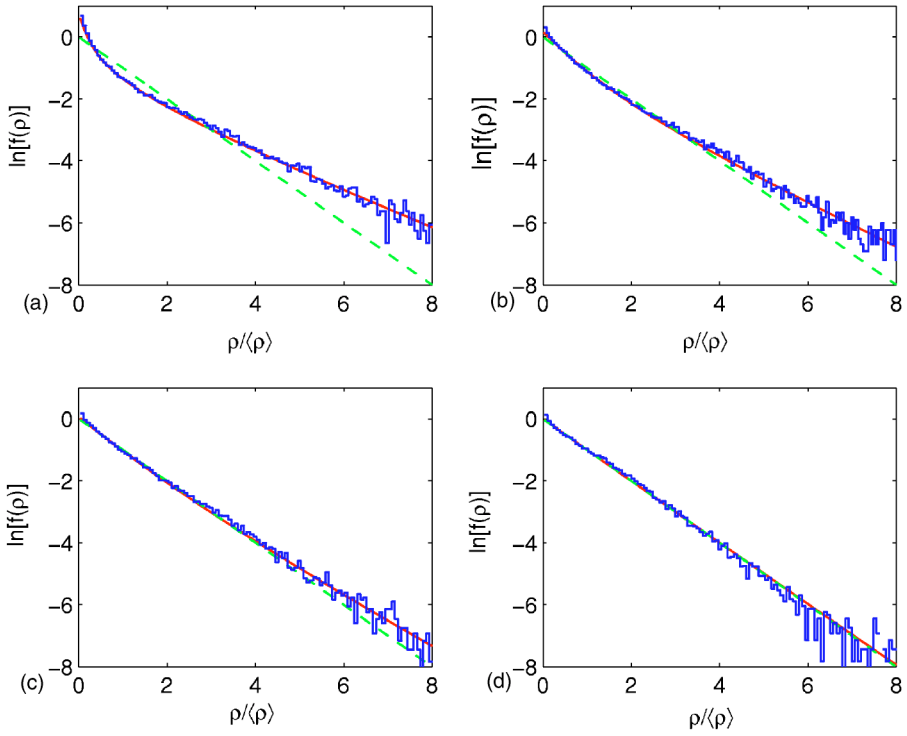

FIG. 5. (Color online) Distribution of the probability density of the quarter Bunimovich billiard mapped onto the resonance *RLC* circuit with the same parameters as in Fig. 4. (a) $R=0.1\ \Omega$, $Q=3162$, $\epsilon=0.2488$; (b) $R=0.3\ \Omega$, $Q=1054$, $\epsilon=0.5308$; (c) $R=0.5\ \Omega$, $Q=632$, $\epsilon=0.6996$; and (d) $R=1\ \Omega$, $Q=316$, $\epsilon=0.9164$. The distribution (13) is shown by the solid line, the Rayleigh distribution $f(\rho)=\exp(-\rho)$ is shown by the dashed line.

To find the distribution of the heat power (15) it is convenient to begin with the characteristic function

$$\Theta(a) = \langle \exp(iaP) \rangle = \int d^2I_x d^2I_y f(I_x', I_y', I_x'', I_y'') \exp(iaR[|I_x|^2 + |I_y|^2]/2). \tag{21}$$

Substituting Eq. (18), we obtain

$$\Theta(a) = -\frac{(\sigma_r^2+\sigma_i^2)^2}{\sigma_r^2\sigma_i^2} \frac{1}{[a+i(\sigma_r^2+\sigma_i^2)/\sigma_r^2][a+i(\sigma_r^2+\sigma_i^2)/\sigma_i^2]}. \tag{22}$$

The knowledge of the characteristic function allows us to find the heat power distribution function

$$f(P) = \frac{1}{2\pi}\int_{-\infty}^{\infty} da\, \Theta(a)\exp(-iaP) = \frac{2\mu}{\nu\langle P\rangle}\exp(-\mu P/\langle P\rangle)\sinh(\nu P/\langle P\rangle), \tag{23}$$

where the formulas (14) take the following form:

$$\mu = \frac{(\sigma_r^2+\sigma_i^2)^2}{2\sigma_r^2\sigma_i^2}, \quad \nu = \frac{(\sigma_r^2-\sigma_i^2)^2}{2\sigma_r^2\sigma_i^2}. \tag{24}$$

For $\sigma_r^2 \approx \sigma_i^2$ the distribution takes the very simple form

$$f(P) = \frac{4P}{\langle P\rangle^2}\exp(-2P/\langle P\rangle). \tag{25}$$

Even for this case the distribution of the heat power differs from the distribution of the probability current [24]. The parameter (12) of the degree of openness of the billiard can be written as

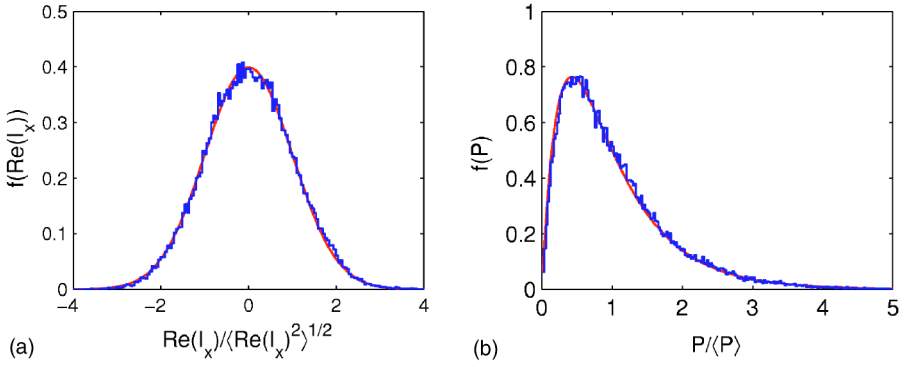

FIG. 6. (Color online) (a) Statistics of the real part of the x component of the electric current I_x compared to the Gaussian distribution (solid line). (b) Statistics of the heat power compared to the distribution (27) (solid line). Here the quarter Bunimovich billiard is taken with $\omega=1.163$ MHz, $R=0.1\ \Omega$, $L=0.1$ mH, $C=1$ nF.

TABLE I. Numerically computed mean values.

ω (MHz)	Wavelength λ in terms of the billiard's width	$\frac{\langle I_x'^2\rangle-\langle I_y'^2\rangle}{\langle I_x'^2\rangle+\langle I_y'^2\rangle}$	$\frac{\langle I_x''^2\rangle-\langle I_y''^2\rangle}{\langle I_x''^2\rangle+\langle I_y''^2\rangle}$	ϵ
0.8611	0.1154	0.095	−0.128	0.2488
1.1623	0.0854	0.056	0.050	0.6103

$$\epsilon^2 = \frac{\sigma_i^2}{\sigma_r^2}. \tag{26}$$

This expression follows from the Schrödinger equation which gives $2\sigma_r^2 = E\sigma_p^2$, $2\sigma_i^2 = E\sigma_q^2$.

Then the heat power distribution function (23) can be written as

$$f(P) = \frac{1+\epsilon^2}{1-\epsilon^2}\left\{\exp\left(-\frac{(1+\epsilon^2)P}{\langle P\rangle}\right) - \exp\left(-\frac{(1+\epsilon^2)P}{\epsilon^2\langle P\rangle}\right)\right\}. \tag{27}$$

The parameter ϵ in Eq. (26) is closely related to the phase rigidity of the wave function, introduced by van Langen *et al.* [27],

$$r = \frac{(\langle p^2\rangle - \langle q^2\rangle)^2}{(\langle p^2\rangle + \langle q^2\rangle)^2} = \left(\frac{1-\epsilon^2}{1+\epsilon^2}\right)^2. \tag{28}$$

In terms of the phase rigidity the power distribution takes the more elegant form

$$f(P) = \frac{1}{r^{1/2}}\left\{\exp\left(-\frac{2}{1+r^{1/2}}\frac{P}{\langle P\rangle}\right) - \exp\left(-\frac{2}{1-r^{1/2}}\frac{P}{\epsilon^2\langle P\rangle}\right)\right\}. \tag{29}$$

This distribution is shown in Fig. 6(b). As can be seen, it nicely describes the numerically computed statistics of the heat power. Introducing the value

$$\sigma_P^2 = \frac{\langle (P-\langle P\rangle)^2\rangle}{\langle P\rangle^2}, \tag{30}$$

one can derive the relation between this parameter and the parameter (26) of the degree of openness

$$\sigma_P^2 = \frac{\epsilon^4+1}{(\epsilon^2+1)^2}. \tag{31}$$

If the quantum system is fully open, $\epsilon=1$, and we have from Eq. (31) that $\sigma_P^2=1/2$. For the other limit of a closed quantum system we obtain $\sigma_P^2=1$.

V. SUMMARY AND CONCLUSIONS

We considered two types of electric circuit networks consisting of *RLC* resonant oscillators, in which the voltages play the role of the quantum wave function. In detail, we considered electric networks with Dirichlet boundary conditions which are equivalent to a quarter of a Bunimovich quantum billiard. However, the electric circuit network has three features that can cause some difference from quantum billiards. These differences are thediscreteness of the resonance circuits, the tolerance of the electric elements, and the resistance of the inductors. We showed numerically that the first two features conceal each other. The resistance of the electric network gives rise to heat that can be described locally by the heat currents. Assuming that the wave function in the billiard can be given as a complex random Gaussian field we derived the distribution of the heat power that describes well the numerical statistics.

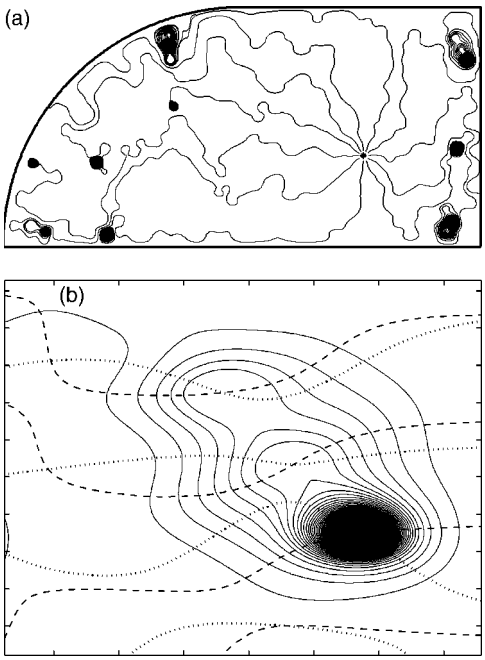

FIG. 7. Top: quantum streamlines in the quarter of the Bunimovich billiard which flow from the point (shown by a star) at which the external ac current is applied. Bottom: zoomed part of top figure. Solid lines show the streamline, and dashed and dotted lines are the nodal lines of the real and imaginary parts of the wave function, respectively. The points at which the nodal lines intersect are centers of vortices [29]. The wave function corresponds to Fig. 4 (right) with the same parameters.

The third feature of the electric network, the resistance, is of principal importance. The resistance of the electric network originates from inelastic interactions of electrons with phonons and other electrons. These interactions give rise to irreversible decoherence processes. With growing resistance, the wave function becomes localized. We studied how the probability density and the probability currents evolve with increasing resistance. As a result, we can conclude that the resistance causes a violation of the equation $\nabla\cdot\mathbf{j}=0$. Indeed, Fig. 7 demonstrates an unusual behavior of the quantum streamlines [28,29] with growing resistance. The quantum streamlines terminate at vortex cores. The vortices serve as sinks for the probability density shown in Fig. 7 (top) as spots. Thus, the resistance of the inductors in the equivalent electric networks is a simple mechanism of the deterioration of the ballistic transport in a manner that is similar to the Büttiker mechanism [30].

ACKNOWLEDGMENTS

A.S. is grateful to K.-F. Berggren for numerous fruitful discussions. We also thank I. Rotter for the discussions. This work is supported by Russian Foundation for Basic Research (RFBR Grants No. 05-02-97713 and No. 05-02-17248). A.S. acknowledges support of the Swedish Royal Academy of Sciences.

[1] G. Kron, Phys. Rev. **67**, 39 (1945).
[2] G. K. Carter and G. Kron, Phys. Rev. **67**, 44 (1945).
[3] J. P. Clerk, G. Giraud, J. M. Laugier, and J. M. Luck, Adv. Phys. **39**, 191 (1990).
[4] J. V. Fyodorov, J. Phys. A **32**, 7429 (1999).
[5] H.-J. Stöckmann, *Quantum Chaos: An Introduction* (Cambridge University Press, Cambridge, U.K., 1999).
[6] H.-J. Stöckmann and J. Stein, Phys. Rev. Lett. **64**, 2215 (1990).
[7] S. Sridhar, Phys. Rev. Lett. **67**, 785 (1991).
[8] H.-D. Gräf, H. L. Harney, H. Lengeler, C. H. Lewenkopf, C. Rangacharyulu, A. Richter, P. Schardt, and H. A. Weidenmüller, Phys. Rev. Lett. **69**, 1296 (1992).
[9] R. L. Weaver, J. Acoust. Soc. Am. **96**, 1005 (1989).
[10] O. Legrand, C. Schimdt, and D. Sornette, Europhys. Lett. **18**, 101 (1992).
[11] P. Bertelsen, C. Ellegaard, and E. Hugues, Eur. Phys. J. B **15**, 87 (2000).
[12] *Handbook of Microwave Measurements*, edited by M. Sucher and J. Fox (Polytechnical Press, New York, 1963).
[13] F. Manolache and D. D. Sandu, Phys. Rev. A **49**, 2318 (1994).
[14] K.-F. Berggren and A. F. Sadreev, in *Mathematical Modelling in Physics, Engineering and Cognitive Sciences*, Vol. 7, pp. 229–239; in *Proceedings of the Conference on Mathematical Modelling of Wave Phenomena, 2002*, edited by B. Nilsson and L. Fishman (Vaxjo University Press, Vaxjo) pp. 133–147.
[15] *Handbook of Mathematical Functions*, edited by M. Abramowitz and I. A. Stegun (Dover, New York, 1970), formula (25.3.30).
[16] S. Iida, H. A. Weidenmüller, and J. A. Zuk, Phys. Rev. Lett. **64**, 583 (1990).
[17] V. N. Prigodin, K. B. Efetov, and S. Iida, Phys. Rev. Lett. **71**, 1230 (1993).
[18] K. Życzkowski and G. Lenz, Z. Phys. B: Condens. Matter **82**, 299 (1991).
[19] G. Lenz and K. Życzkowski, J. Phys. A **25**, 5539 (1992).
[20] E. Kanzieper and V. Freilikher, Phys. Rev. B **54**, 8737 (1996).
[21] R. Pnini and B. Shapiro, Phys. Rev. E **54**, R1032 (1996).
[22] H. Ishio, A. I. Saichev, A. F. Sadreev, and K.-F. Berggren, Phys. Rev. E **64**, 056208 (2001).
[23] M. Barth and H.-J. Stöckmann, Phys. Rev. E **65**, 066208 (2002).
[24] A. I. Saichev, H. Ishio, A. F. Sadreev, and K.-F. Berggren, J. Phys. A **35**, L87 (2002).
[25] B. D. Popovic, *Introductory Engineering Electromagnetics* (Addison-Wesley, Reading, MA, 1971).
[26] A. M. Dykhne, Sov. Phys. JETP **59**, 110 (1970).
[27] S. A. van Langen, P. W. Brouwer, and C. W. J. Beenakker, Phys. Rev. E **55**, R1 (1997).
[28] A. F. Sadreev and K.-F. Berggren, Phys. Rev. E **70**, 026201 (2004).
[29] K.-F. Berggren, A. F. Sadreev, and A. A. Starikov, Phys. Rev. E **66**, 016218 (2002).
[30] M. Büttiker, Phys. Rev. B **33**, 3020 (1986).